

Wet chemical synthesis of $\text{La}_{9.83-x}\text{Sr}_x\text{Si}_6\text{O}_{26+\delta}$ ($0 \leq x \leq 0.50$) powders, characterization of intermediate and final products

Kioupis D., Argyridou M., Gaki A., Kakali G.*

(National Technical University of Athens, School of Chemical Engineering, 9 Heroon Polytechniou St., Athens 15773, Greece)

Received 28 March 2014; revised 5 November 2014

Abstract: In this paper we reported the preparation and extensive characterization of $\text{La}_{9.83-x}\text{Sr}_x\text{Si}_6\text{O}_{26+\delta}$ ($0 \leq x \leq 0.50$) precursors, intermediate and final products. The sintering reactions, the phase formation, the structure as well as the powders' morphology were studied by means of thermogravimetric analysis, X-ray diffraction (XRD), Fourier-transform infrared spectroscopy (FTIR) and scanning electron microscopy (SEM). Moreover, the effect of stoichiometry on precursor's structure and morphology as well as on intermediate and final products was reported. As was concluded pure $\text{La}_{9.83}\text{Si}_6\text{O}_{26+\delta}$, $\text{La}_{9.38}\text{Sr}_{0.45}\text{Si}_6\text{O}_{26+\delta}$ and $\text{La}_{9.33}\text{Sr}_{0.50}\text{Si}_6\text{O}_{26+\delta}$ could be prepared after sintering at 1400 °C for 20 h while $\text{La}_{9.68}\text{Sr}_{0.15}\text{Si}_6\text{O}_{26+\delta}$ and $\text{La}_{9.53}\text{Sr}_{0.30}\text{Si}_6\text{O}_{26+\delta}$ compounds contained minor traces (<3.5%) of $\text{La}_2\text{Si}_2\text{O}_7$ secondary phase. Concerning the synthesis, there have been no previous reports on the preparation of pure $\text{La}_{9.83}\text{Si}_6\text{O}_{26+\delta}$, $\text{La}_{9.38}\text{Sr}_{0.45}\text{Si}_6\text{O}_{26+\delta}$ and $\text{La}_{9.33}\text{Sr}_{0.50}\text{Si}_6\text{O}_{26+\delta}$ compounds. The final powders consisted of spherical particles and an increase of Sr content seemed to inhibit sintering phenomena. The existence of interstitial oxygen at intermediate crystallographic positions of apatite structure had great effect on SiO_4 sub-structure distortion. The increase of Sr content led to a major reduction of interstitial oxygen quantity and the refutation of silicon tetrahedron distortion.

Keywords: lanthanum silicates; synthesis; modified Pechini method; characterization; rare earths

Apatite type lanthanum silicates (ATLS) with general formula $\text{La}_{9.33+x}\text{Si}_6\text{O}_{26+\delta}$ are a newly reported family of compounds^[1,2]. These compounds exhibit high ionic conductivity combined with low activation energy values at intermediate temperatures (500–700 °C) and are considered as promising electrolytes for IT-SOFCs. For example, the conductivity of Mg-doped apatite $\text{La}_{10}\text{Si}_{5.8}\text{Mg}_{0.2}\text{O}_{26.8}$ ^[3] is much higher than those of the well-established SOFC electrolyte, YSZ^[4], at 500 °C (14×10^{-3} S/cm for $\text{La}_{10}\text{Si}_{5.8}\text{Mg}_{0.2}\text{O}_{26.8}$ compound versus 1.1×10^{-3} S/cm at 500 °C). ATLS own a hexagonal crystal structure which is built from isolated tetravalent $[\text{SiO}_4]^{4-}$ tetrahedrons with the La^{3+} cations located into seven- and nine-coordinate cavity sites. This three-dimensional framework is arranged to form distinct oxide ion and La channels which cross the structure parallel to the *c*-axis. The former are responsible for the high oxide ion conduction. It is found that the structure of these materials permits an unusually broad range of cation doping, on both La and Si sites, with the observed conductivity being very sensitive to the doping regime and cation/anion nonstoichiometry^[3,5–8]. It is well established that fully stoichiometric systems e.g., $\text{La}_8\text{Sr}_2\text{Si}_6\text{O}_{26}$ have much lower conductivities and higher activation energies than systems containing either cation vacancies ($\text{La}_{9.33}\text{Si}_6\text{O}_{26}$) or oxygen excess ($\text{La}_9\text{Sr}_1\text{Si}_6\text{O}_{26.5}$)^[5,9–11]. The highest conductivities are found for the samples containing excess

oxygen suggesting that oxide ion conduction proceeds via an interstitial oxide ion mechanism^[11–15]. Lately, research groups focus their studies on compounds with both cation vacancies and oxygen excess, in an attempt to further enhance their ionic conductivity^[16–18].

The common synthetic route that is used for the preparation of ATLS is based on solid state reactions^[19–21]. This route possesses many drawbacks such as inability in controlling the crystalline growth, composition non-homogeneity and grain size non-uniformity. In order to overcome the aforementioned problems, many research groups investigated the application of alternative synthetic routes such as sol-gel synthesis^[22–26], coprecipitation^[27], glycine-nitrate combustion^[28], freeze drying^[4] and high energy ball milling^[29]. One of the most successful and versatile synthetic routes for the preparation of ceramic oxides is Pechini method^[30,31], although it has so far found little use in the synthesis of ATLS powders^[32].

In this work we reported the synthesis of pure $\text{La}_{9.83-x}\text{Sr}_x\text{Si}_6\text{O}_{26+\delta}$ ($0 \leq x \leq 0.50$) via a modified Pechini method^[33,34]. The effect of stoichiometry on precursor's structure and morphology as well as on intermediate and final products was studied. Moreover, we reported the extensive characterization of intermediate and final products which were examined by means of thermogravimetric analysis (TG), X-ray diffraction (XRD), Fourier

* Corresponding author: Kakali G. (E-mail: kakali@central.ntua.gr; Tel.: +302107723270)

transform infrared spectroscopy (FTIR) and scanning electron microscopy (SEM). Concerning the synthesis there are no previous reports on the preparation of single phase $\text{La}_{9.83}\text{Si}_6\text{O}_{26+\delta}$, $\text{La}_{9.38}\text{Sr}_{0.45}\text{Si}_6\text{O}_{26+\delta}$ and $\text{La}_{9.33}\text{Sr}_{0.50}\text{Si}_6\text{O}_{26+\delta}$ compounds.

1 Materials and methods

1.1 Synthesis procedure

La_2O_3 (Aldrich 99.9%), SrCO_3 (Aldrich 99.9%) and SiO_2 sol in ethylene glycol (Alfa Aesar 30% w/w) were used as the starting materials. All resins were prepared according to the following procedure. First, the amount of citric acid monohydrate (molar ratio of acid to total cations of target compound equals to 2:1) was dissolved in deionised water. Stoichiometric amounts of all cation sources were added along with 40 mL HNO_3 (65% w/w) and the solution was stirred at 45 °C for 30 min until complete dissolution occurred. Ethylene glycol (the molar ratio of ethylene glycol to citric acid was adjusted to 3) was then added and the clear resulting solution was continuously stirred at 60 °C for at least 30 min. The molar ratio of NO_3^- :EG:CA was adjusted to 2.6:3:1. The as-prepared clear solution was subsequently heated in a modified household microwave (MW) oven for 15 min in order to achieve evaporation of excess water and accelerate the polyesterification reaction. The solutions were heated at 150 °C to evaporate till a puff brown resin formed, which was then ground and calcined at various temperatures in the range 600–1400 °C for 3–20 h.

The samples were named as LsSX where L=La, s=Sr, S=Si and X=100× corresponding to the Sr-dopant's level $x=0, 0.15, 0.3, 0.45$ and 0.5 (LsS45: $\text{La}_{9.83-0.45}\text{Sr}_{0.45}\text{Si}_6\text{O}_{26+\delta}$).

1.2 Characterization methods

Thermogravimetric analysis (TG) was applied in order to record the calcination reactions of the powder precursors, using a Mettler Toledo 851 instrument. The samples were heated at a temperature range from 25 to 1200 °C at a constant rate of 10 °C/min in an atmosphere of air.

The phase distribution of the powders was investigated by X-ray diffraction, on a Siemens D-5000 diffractometer with $\text{Cu K}\alpha_1$ radiation ($\lambda=0.15405$ nm), operating at 40 kV, 30 mA. The data were collected in a 2θ range 15°–55°, with step size 0.02° and time 3 or 20 second per step.

FTIR measurements were carried out using a Fourier transform infrared spectrophotometer (Perkin Elmer 880). The FTIR spectra, in the wavenumber range from 370 to 4000 cm^{-1} , were obtained by the KBr pellet technique. The pellets were prepared by pressing a mixture of the sample and dried KBr (sample: KBr approximately 1:200) at 6 t/cm². Precursors and intermediate products

till 800 °C were measured with the use of ATR attachment in the form of powders and wavenumber range 600–4000 cm^{-1} .

The morphology of the products was examined using a JEOL JSM-5600 scanning electron microscope equipped with an OXFORD LINK ISIS 300 energy dispersive X-ray spectrometer (EDX).

2 Results and discussion

2.1 Thermogravimetry measurements

Fig. 1 shows the DTG curves of the precursors. All curves are quite similar. The first mass loss up to 160 °C is related to moisture loss (step 1). The major mass loss takes place at 160–580 °C in two steps. The first one (~160–390 °C) can be attributed to the decomposition of the organic polymer network (step 2) and the second one (~390–580 °C) to the burnout of the organic matter (step 3). As the Sr content increases the mass loss in the step 3 becomes more pronounced. At the same time in Sr-rich samples the first stage of polymer decomposition (step 2) is shifted at higher temperatures (of 40 °C maximum). This can be attributed to the substitution of trivalent La cations by the divalent Sr cations leading to excess of citric acid in the polymeric resin and the formation of compact and linear polymers which require higher decomposition temperatures. The next mass loss at around 580–710 °C can be assigned to the formation and decomposition of carbonates and oxocarbonates (step 4)^[35–37]. This was also confirmed by XRD measurements. The small mass loss at 710 to 850 °C can be attributed to the burnout of the residual carbon and the formation of the apatite phase (step 5). This assumption was also confirmed by the FTIR spectra of the compounds at the same temperature where the characteristic vibrations of silicon tetrahedron groups are observed for the first time.

2.2 FTIR spectroscopy

The FTIR spectra of the dried resins are shown in Fig. 2. The band at 2940 cm^{-1} is typical of the C–H stretching vibration, while the bands around 1720, 1150 and 1080

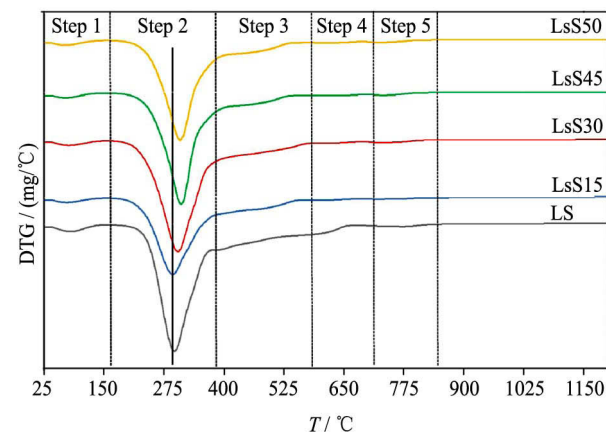


Fig. 1 DTG curves of the precursors

Download English Version:

<https://daneshyari.com/en/article/1259121>

Download Persian Version:

<https://daneshyari.com/article/1259121>

[Daneshyari.com](https://daneshyari.com)